QUATERNARY RESEARCH 44, 303–316 (1995)

The Growth and Decay of the Late Weichselian Ice Sheet in Western Svalbard and Adjacent Areas Based on Provenance Studies of Marine Sediments

ANDERS ELVERHØI AND ESPEN S. ANDERSEN
University of Oslo, Department of Geology, P.O. Box 1047, Blindern N-0316 Oslo, Norway

TROND DOKKEN
University of Tromsø, Department of Biology and Geology, N-9037, Tromsø, Norway

DIERK HEBBELN
Universität Bremen, Fachbereich Geowissenschaften, Postfach 330440, D-28334 Bremen, Germany

ROBERT SPIELHAGEN
GEOMAR, Research Center for Marine Geosciences, Wischhofstrasse, 1-3, D-24148 Kiel, Germany

JOHN INGE SVENDSEN
University of Bergen, Center for Studies of Environment and Resource, Høyteknologisenteret, N-5020 Bergen, Norway

MARIT SØRFLATEN
University of Oslo, Department of Geology, P.O. Box 1047, Blindern N-0316 Oslo, Norway

ARNT RØRNES AND MORTEN HALD
University of Tromsø, Department of Biology and Geology, N-9037, Tromsø, Norway

AND

CARL FREDRIK FORSBERG
Norwegian Polar Institute, Middelthunsgt. 29, P.O. Box 5072, Majorstua 0301, Oslo, Norway

Received December 11, 1994

The history of the Late Weichselian northwestern Barents Shelf, including western Svalbard, has been investigated by provenance/sedimentologist studies of five cores from the continental shelf and slope west of Svalbard. The chronostratigraphy of the cores is based on AMS ^{14}C dates and oxygen isotope analyses. Interpretations of the cores suggest that the ice sheets of western Svalbard and northwestern Barents Sea experienced advances and retreats in two steps. The first significant ice advance beyond the present coastline occurred ca. 22,000 ^{14}C yr B.P. and was followed by an ice advance to the shelf edge ca. 18,000 ^{14}C yr B.P. Ice recession from the outer shelf and the southwestern Barents Sea began 14,800 ^{14}C yr B.P. and was followed by a second ice recession between 13,000 and 12,000 ^{14}C yr B.P. during which ice withdrew from the inner shelf. A minor readvance of the ice sheet on the shelf west of Svalbard occurred close to 12,400 ^{14}C yr B.P. The first deglaciation event was associated with release of icebergs containing ice-rafted detritus, while the later episode also included significant amounts of meltwater and fine-grained sediment.

INTRODUCTION

The terrestrial record on Svalbard has provided evidence for three Weichselian advances of the Svalbard–Barents Sea Ice Sheet (Mangerud and Svendsen, 1992). Additional information on the timing of these advances has been provided from deep-sea cores from the Norwegian-Greenland Sea. The two last glacial advances (Middle and Late Weichselian), in particular have been identified by an increased influx of terrigenous material (Hebbeln, 1992). However, due both to the limited stratigraphic resolution of deep-sea cores and to the fragmentary onshore geologic record, it has been difficult to determine either the exact timing of the onset or the culmination of the glacier advances during these two stades. In order to resolve this problem, several high-resolution sediment cores from the continental slope and shelf west of Svalbard have been analyzed. As a result, it is now possible to outline a more detailed glacial history of the Svalbard-Barents Sea Ice Sheet throughout the Late Weichselian (Hebbeln *et al.*, 1994).

In this paper we present new evidence on the glacial history of the Svalbard archipelago and the northwestern Barents Sea during the Late Weichselian, based on the marine sedimentary record. Emphasis is given to the ice-sheet history of the western part of the Svalbard archipelago because it is well reflected in the sediment cores along a continent–sea transect from the Isfjorden to the adjacent continental shelf and upper slope to the west (Fig. 1, Table 1). In addition, cores from the lower

0033-5894/95 $12.00

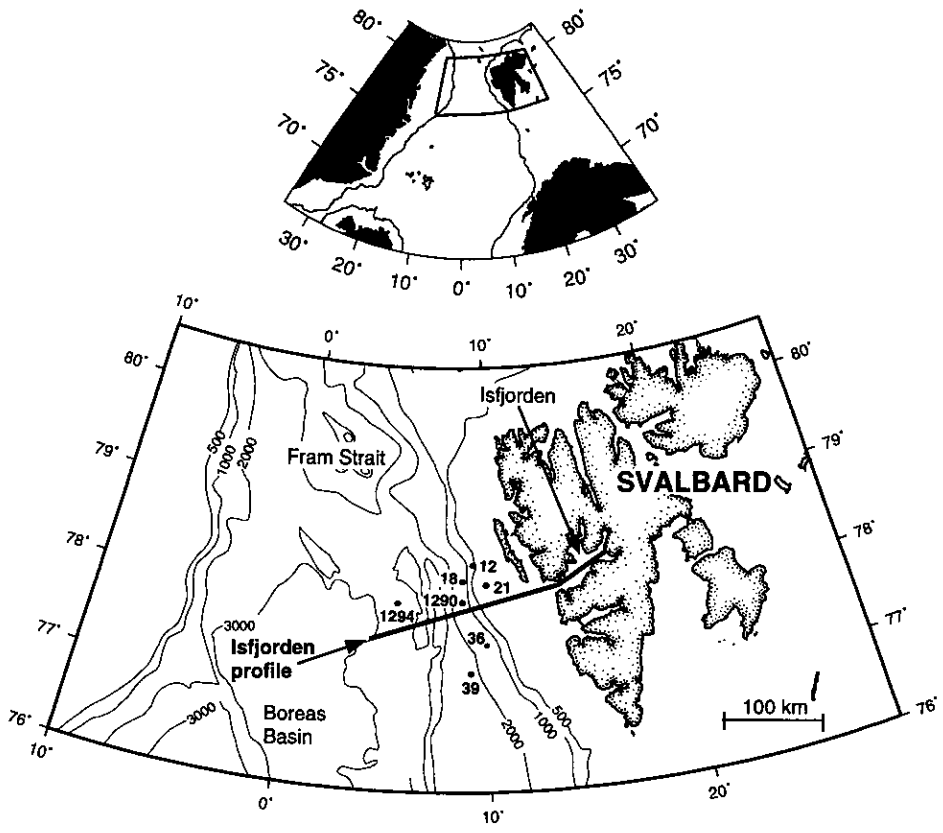

FIG. 1. Map showing the core locations (see also Table 1) (Bathymetric contour interval: 1000 m).

continental slope and the adjacent deep sea are used to monitor the broader glacial signal of the Svalbard and northwestern Barents Sea Ice Sheet.

PHYSIOGRAPHY

The Svalbard margin is characterized by a relatively narrow shelf, between 60 and 85 km wide, and a steep (up to 5°) continental slope. The shelf is characterized by shallow banks, with water depths of <100 m and troughs representing a continuation of the fjords. Situated off the mouth of the troughs are well-defined submarine fans that continue downslope toward the mid-oceanic ridge (Fig. 1). It has been demonstrated from seismic profiles and sediment samples that some of the banks on the shelf are covered by till and some represent well-defined moraine ridges (Svendsen *et al.*, 1992; Andersen *et al.*, 1994). Although the inner shelf is covered by a thin (<10 m) veneer of sediment overlying bedrock (Andersen *et al.*, 1994; Elverhøi *et al.*, 1995), the sediment thickness increases significantly, up to 700 m, toward the outer shelf.

Modern surface waters along the western margin of Svalbard are strongly influenced by the north-flowing West-Spitsbergen Current, an extension of the North Atlantic and Norwegian currents (Hopkins, 1991). The hydrographic regime along the western coast of Svalbard is also affected by the East Spitsbergen Current, a coastal current that supplies cold polar water and winter sea ice from the northwestern Barents Sea and eastern Svalbard (Vinje, 1985).

TABLE 1
Core Locations and Water Depths

Core	North latitude	East longitude	Water depth (m)	Sample recovery (cm)
NP90-12/PC(1)	78°24.47′	09°24.88′	628	335
NP20-21	78°11.30′	09°56.56′	322	209
NP90-18/PC(1)	78′14.18′	08°47.82′	1444	630
NP90-36/PGC(1)	77°37.04′	09°56.18′	1360	380
NP90-39/PC(1)	77°49′	09°05.58′	2119	600
1290-4GC	78°00.8′	8°43.2′	1522	505
1294-4GC	77°59.9′	5°22.3′	2668	616

METHODS

Radiocarbon Dating and Stable Oxygen Isotope Analysis

The stratigraphic interpretation of the investigated cores is based on radiocarbon dating using accelerator mass spectrometry (AMS) and stable oxygen isotope analyses (Table 2). All AMS dates are corrected for ^{13}C and a reservoir age of 440 yr (Mangerud and Gulliksen, 1975).

Stable oxygen isotope measurements also were performed on the planktic *N. pachyderma* (sin.). All the NP-90 cores were measured at the Norwegian Geological Mass Spectrometer (GMS) laboratory at the University of Bergen (Dokken, 1995),

TABLE 2
^{14}C Dates and Laboratory Identification Numbers (U/TUa, Th. Swedberg Laboratory, Uppsala; ETH, ETH Zurich Laboratory)

Core	Mean depth (cm)	Corrected ^{14}C age (yr B.P.) and 1σ error	Laboratory number	Material type
NP90-12	30	11,940 ± 320	TUa-562	*N. pachyderma*
NP90-12	192	13,315 ± 100	TUa-846	*N. pachyderma*
NP90-12	219.5	14,760 ± 160	TUa-563	*N. pachyderma*
NP90-12	262.5	17,245 ± 130	TUa-564	*N. pachyderma*
NP90-18	182.5	19,635 ± 230	Ua-3270	*N. pachyderma*
NP90-18	182.5	19,645 ± 210	Ua-3271	*N. pachyderma*
NP90-21GC	15	3640 ± 150	TUa-361	*N. pachyderma*
NP90-21GC	40	12,510 ± 90	TUa-211	Yoldiel.lentic
NP90-21GC	60	12,485 ± 110	TUa-358	Yoldiel.lentic
NP90-21GC	89	12,920 ± 110	TUa-191	Mollusc
NP90-21GC	140	13,235 ± 110	TUa-360	*N. labradoricum*
NP90-21GC	145	13,040 ± 110	TUa-192	Mollusc
NP90-21GC	152	12,855 ± 130	TUa-438	*N. labradoricum*
NP90-21GC	159	14,815 ± 180	TUa-359	*N. pachyderma*
NP90-21GC	160	14,595 ± 90	TUa-855	*N. pachyderma*
NP90-21GC	162	14,710 ± 120	TUa-856	*N. pachyderma*
NP90-36	18.5	7975 ± 110	TUa-842	*N. pachyderma*
NP90-36	64.5	8855 ± 80	TUa-843	*N. pachyderma*
NP90-36	160	11,730 ± 110	TUa-844	*N. pachyderma*
NP90-36	331	15,595 ± 130	TUa-845	*N. pachyderma*
NP90-39	48.5	7855 ± 90	TUa-343	*N. pachyderma*
NP90-39	123.5	13,100 ± 120	TUa-558	*N. pachyderma*
NP90-39	126.5	14,495 ± 120	TUa-561	*N. pachyderma*
NP90-39	128.5	15,135 ± 110	TUa-342	*N. pachyderma*
NP90-39	160.5	19,375 ± 120	TUa-557	*N. pachyderma*
NP90-39	186	21,185 ± 160	TUa-559	*N. pachyderma*
NP90-39	246	23,080 ± 200	TUa-341	*N. pachyderma*
NP90-39	269	29,605 ± 650	TUa-560	*N. pachyderma*
1290-4	307.5	18,860 ± 150	ETH-9914	*N. pachyderma*
1290-4	360	22,610 ± 200	ETH-9915	*N. pachyderma*
1294-4	7	5045 ± 70	ETH-9917	*N. pachyderma*
1294-4	40	16,230 ± 120	ETH-9921	*N. pachyderma*
1294-4	55	18,160 ± 150	ETH-9918	*N. pachyderma*
1294-4	75	22,150 ± 200	ETH-9916	*N. pachyderma*
1294-4	85	26,340 ± 270	ETH-9920	*N. pachyderma*
1294-4	101	28,210 ± 310	ETH-9919	*N. pachyderma*

while the other cores were analyzed at the Department of Geosciences, University of Bremen (D. Hebbeln, and G. Wefer, unpublished data).

Samples were obtained on 1- to 4-cm-thick sediment slices depending on stratigraphic resolution. Age determination between dated levels were based on linear interpolation using the assumption of constant sedimentation rates.

Paleoenvironmental and Provenance Parameters

Although 90% of the sediment transported by sea ice is <63 μm in size (Pfirman *et al.*, 1989), relatively large amounts of coarser sediment (sand and gravel) can be transported and deposited by icebergs (Dowdeswell and Dowdeswell, 1989). Therefore, terrigenous particles with a grain size >500 μm found in marine muds most likely represent iceberg-rafted debris (IRD). Increased IRD flux is assumed to reflect increased rates of iceberg calving.

Initially, clasts were separated into 25 lithologic classes, using binocular microscope and thin section analyses. Later, however, these classes were combined into four groups: clastic sedimentary, nonclastic sedimentary, crystalline, and monocrystalline rock fragments.

Accumulation Rates

The calculation of bulk accumulation rate (AR_{bulk}), accumulation rate of grains >500 μm (AR_{IRD}), and accumulation rate of the different lithologic groups ($AR_{clastic}$, $AR_{nonclastic}$, $AR_{cryst.}$, and $AR_{monocryst.}$) follow procedures detailed by Ehrmann and Thiede (1985).

Total Organic Carbon Content (C_{org}) and C/N-ratio, Carbonate Content

The organic carbon (HCl-treated) and total nitrogen contents of the sediments were measured using a HEREAUS CHN-O-RAPID elementary analyzer. Total nitrogen values include organic as well as inorganic nitrogen. Here the C_{org}/N_{tot} ratio is

used to give primary information about the relative amount of reworked organic matter in the marine sediments, where higher C/N-ratios reflect a higher content of reworked organic material (Emerson and Hedges, 1988).

Total carbon contents of untreated samples were measured using a LECO 5344 analyzer and a HEREAUS CHN-O-RAPID elementary analyzer. Carbonate contents were calculated by multiplying the difference between the contents of C_{total} and C_{org} with 8.33 (mole-weight ratio of $CaCO_3$-to-C).

Clay Minerals

Clay mineral identification and semiquantitative calculations of the clay minerals followed the outlines of Pearson (1990).

Palynological Analyses

The palynomorphs were prepared from bulk samples, taken at 1-cm intervals in selected levels of three cores, and analyzed by T. Bjærke, StratLab, Norway (Bjærke, 1993).

RECONSTRUCTION OF THE LATE WEICHSELIAN HISTORY OF THE SVALBARD-NORTHWESTERN BARENTS SEA ICE SHEET

Six time intervals have been identified based on important changes observed in the investigated cores (Fig. 2, Table 3). The various intervals represent characteristic events on the Svalbard margin during the Late Weichselian glaciation. In general, the analyzed sediments can be divided into four lithofacies, including structureless, laminated, layered, and bioturbated muds (Andersen, 1995). All facies are associated with pebbles, except for the laminated mud which is generally free of clasts.

27,000 to 23,000 ^{14}C yr B.P.

The first period is characterized by a low influx of iceberg-rafted sediment and low accumulation rates (Fig. 3a). The reworked palynomorphs in core NP90-39 (Fig. 4b) are derived from Triassic rocks, widely exposed on eastern Svalbard and in the northern Barents Sea (Fig. 5). The sediments also contain palynomorphs of Late Cretaceous age; rocks of this age crop out only in the eastern part of the Barents Sea region (Fig. 5). The clay mineral assemblage consists of a mixture of smectite (with randomly mixed layers of illite and smectite), kaolinite, illite, and chlorite (Andersen, 1995). Such an assemblage is typical of most Mesozoic rocks on Svalbard and also of the Late Quaternary sediments analyzed from the floor of the Barents Sea (Bjørlykke *et al.*, 1978, Elverhøi *et al.*, 1989).

Due to low accumulation rates (fine-grained sediment as well as IRD), we suggest that during this time interval there was no grounded ice in the Barents Sea and that the glaciers on Svalbard were located within the fjords along the western coast of Spitsbergen. The eastern islands of the Svalbard archipelago (Fig. 1) could have been covered by grounded ice, since Triassic rock particles are present in the cores.

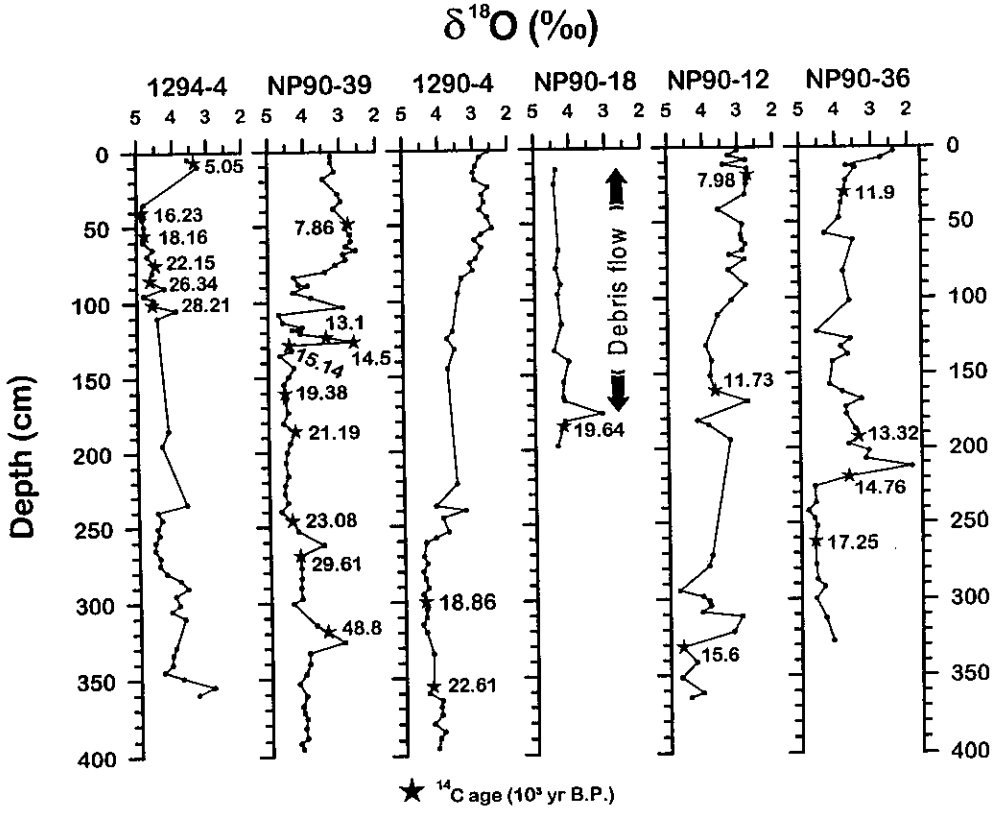

FIG. 2. Plot of $\delta^{18}O$ versus depth, including the AMS dates. Decreasing water depth toward right (see also Table 2).

TABLE 3
Definition of Time Intervals and Critical Events

Time interval (^{14}C yr B.P.)	Event
27,000–23,000	Low sediment input and first period with open water conditions (type A)
23,000–19,400	First event with high terrestrial input of hemipelagic sediments (type B)
19,400–14,800	Second stage with open water, (type A)
14,800–13,000	First stage of ice recession (type B), meltwater peak
13,000–11,000	Second stage of deglaciation with increased melting and temporary glacial readvance
11,000–9500	Younger Dryas event and final deglaciation of the remaining ice sheet

Note. The types A and B refer to alternating sequences in the slope and deep sea cores of low accumulation rate and intermediate carbonate content (>10%) and low C/N ratios (<7) and TOC contents (<0.5%) (type A) and high accumulation rate, low carbonate content (5%) and high C/N ratios (>10%) and TOC contents (>0.5%) (type B).

23,000 to 19,400 ^{14}C yr B.P.

Soon after 23,000 ^{14}C yr B.P. the input of organic matter increased as well as the C/N ratio, indicating a major shift in provenance to a region rich in organic matter (Fig. 4). In the early part of this interval, the palynomorphs are dominated by Triassic and Early Cretaceous assemblages, with additional input of Cretaceous palynomorphs (Fig. 4), indicative of a provenance from the northern and eastern Barents Sea, respectively (Fig. 5). High input of organic-rich sediments is also demonstrated by the presence of palynomorphs characteristic of Late Jurassic "Hot Shale" (Fig. 4b). Such rocks are found on Svalbard (Agardhfjellet Formation), and equivalent rocks occur on Spitsbergenbanken and the central Barents Sea, in a corridor between Cretaceous (K1) and Triassic-Early Jurassic (TR-J1) rocks (Fig. 5).

A major change in sediment source was also observed in the clay mineral composition (Fig. 6). The randomly mixed illite-smectite minerals, characteristic of the period between 27 and 23 ka, are replaced by ordered illite-smectite mix-layered minerals and an increase in the kaolinite content (Andersen, 1995) (Fig. 6). The latter clay mineral assemblage is frequently found in organic-rich Upper Jurassic clasts and Late Quaternary sediments on Spitsbergenbanken and in the central Barents Sea (Bjørlykke *et al.*, 1978).

Based on the high influx of Spitsbergenbanken-type sediment (Fig. 5), it is assumed that during this time interval the ice sheet extended beyond the present coastline and onto the relatively shallow shelf of the northwestern Barents Sea (Fig. 1). The expanding ice sheet is likely to have supplied large amounts of fine-grained terrigenous sediment both to the continental slope and the deep sea (Andersen, 1995). In core NP90-39, an increase in the IRD input (grains >500 μm) began 21,500 ^{14}C yr B.P., approximately 1500 yr later than the onset of high input of the finer grained fractions (Fig. 3a). The increase of IRD is interpreted to reflect an increased calving rate of the ice sheet that occurred when it reached deeper parts of the Barents Sea, given that iceberg production rate is sensitive to increasing water depth (Hughes, 1992).

19,400 to 14,800 ^{14}C yr B.P.

At 19,400 ^{14}C yr B.P. the sedimentary record shifted back to one similar in composition to that deposited between 27,000 and 23,000 yr ^{14}C B.P. A considerable amount of IRD exists in the sediments of this period, but there is an obvious change to a dominance of crystalline grains instead of sedimentary rock fragments in the cores from the deeper parts of the slope (Fig. 3a). One source of the crystalline clasts may have been the western coastal zone along the Svalbard archipelago (Fig. 5). However, due to the limited exposure of these rocks, it is unlikely that Svalbard is the only source area. We therefore suggest that a fraction of the crystalline grains originated in Fennoscandia and was transported by a northward drift of iceberg from the south. Evidence for the northward transport of icebergs during this period is the existence of chalk fragments in this layer (Fig. 3a). Such chalk fragments are diagnostic of North Sea tills and southern North Sea bedrock (e.g., Spielhagen, 1991).

The change in IRD composition at 19,400 yr ^{14}C B.P. is also reflected by lower C_{org} contents and C/N ratios, indicating reduced erosion of Mesozoic rocks from Svalbard, even though the reworked palynomorphs still indicate a sediment supply from the Svalbard-Barents Sea (Fig. 4). A palynomorph assemblage of early Tertiary age is also connected with this interval. Such early Tertiary rocks are not present on Svalbard but have been found in the outer part of the Bear Island Trough (Fig. 5), possibly reflecting an ice advance to this region.

The accumulation rates, except for the fan core NP90-18, are generally reduced by a factor of five in relation to the preceding time interval. This seems to be inconsistent with an ice advance to the shelf during the glacial maximum (e.g., Mangerud and Svendsen, 1992), when an increase in sediment input to the slope would be expected. However, cores from the Isfjorden Fan indicate deposition of debris flows during the glacial maximum (Andersen, 1995). The maximum position of the ice front is indicated by a well-defined moraine ridge in the southern part of the Isfjorden Trough (Andersen *et al.*, 1994) and similar ridges located farther south along the Svalbard–Barents Sea margin (Elverhøi *et al.*, 1993). Observed glacially fluted surfaces in the southern Barents Sea (Solheim *et al.*, 1990) and the subcrop of Tertiary rocks (Fig. 5) indicate a minimum extension of the ice front during the Late Weichselian glacial maximum.

14,800 to 13,000 ^{14}C yr B.P.

Several AMS dates from glacialmarine sediments just above the till in core NP90-21 indicate that the Late Weichselian Ice Sheet retreated from the shelf break west of Isfjorden ca. 14,800 ^{14}C yr B.P. or shortly before (Fig. 3d). At the same time, the δ^{18}O records from the continental slope (Figs. 2 and

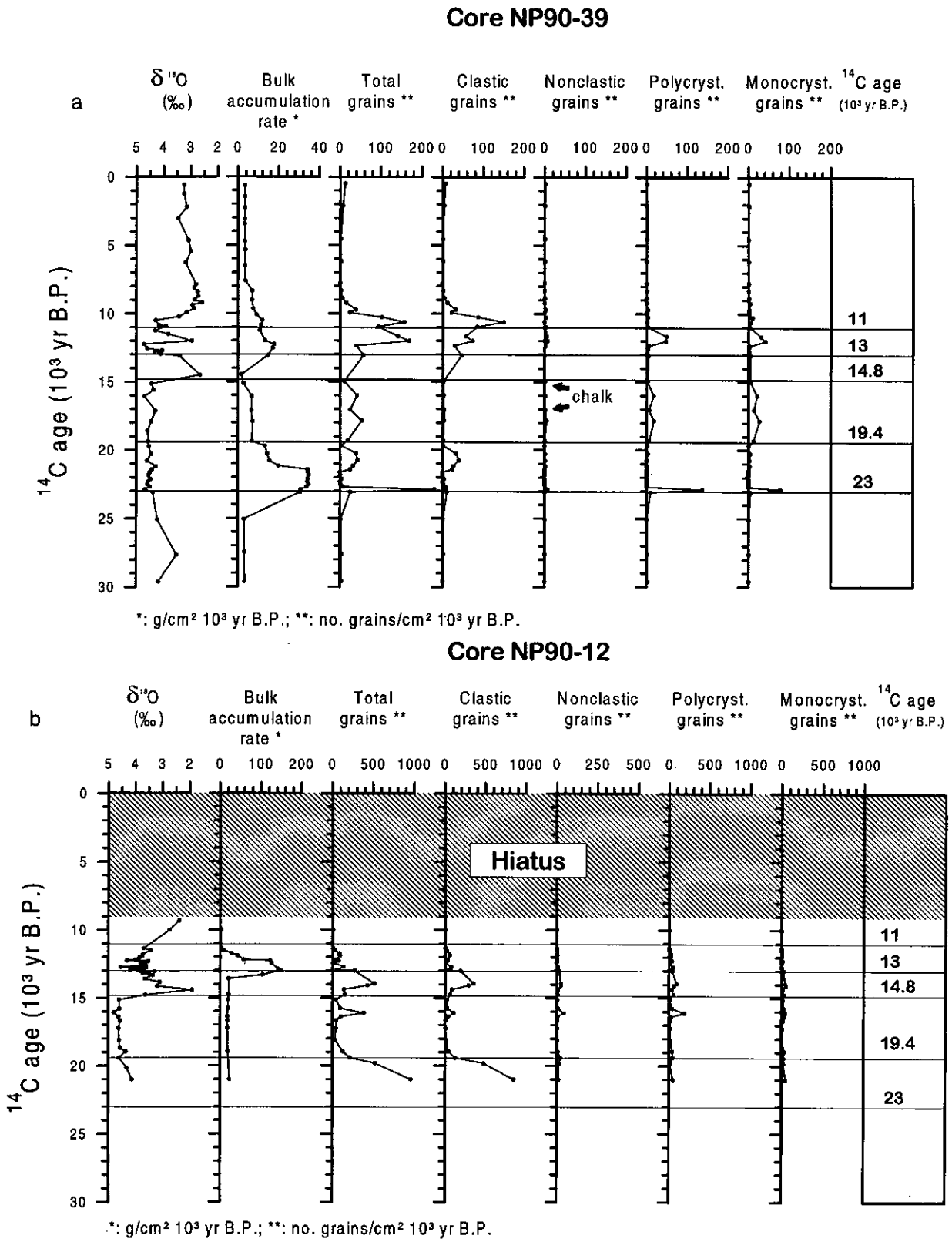

FIG. 3. Plot of bulk accumulation rate (BAR), accumulation rate of grains >500 μm, and accumulation rate of clastic, nonclastic, polycrystalline, and monocrystalline grains. (a) NP90-39, (b) NPP90-12, (c) NP90-36, and (d) NP90-21. Note that an accumulation rate of 10 g/cm² · 1000 yr ≈ a sedimentation rate of 10 cm/1000 yr.

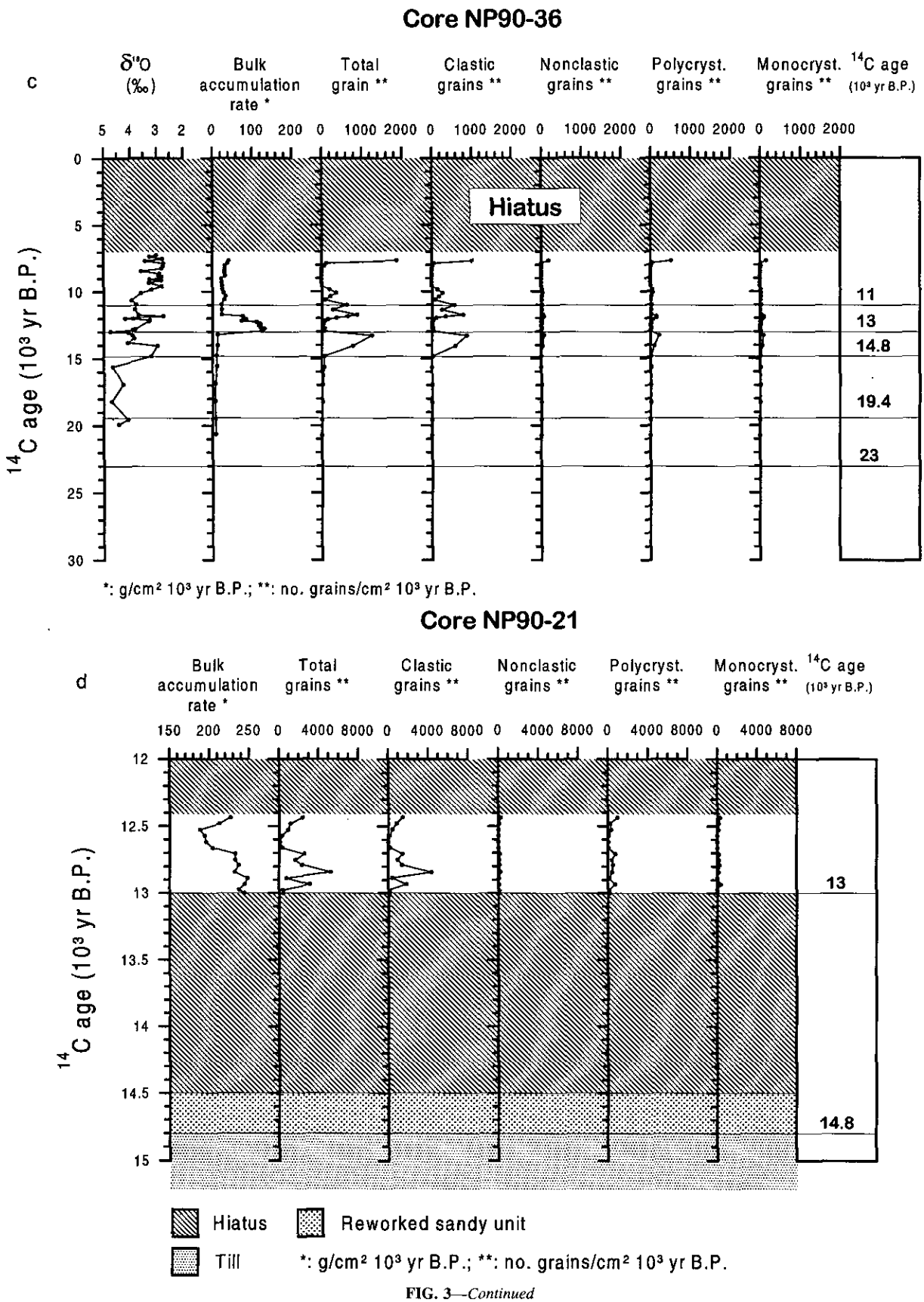

FIG. 3—*Continued*

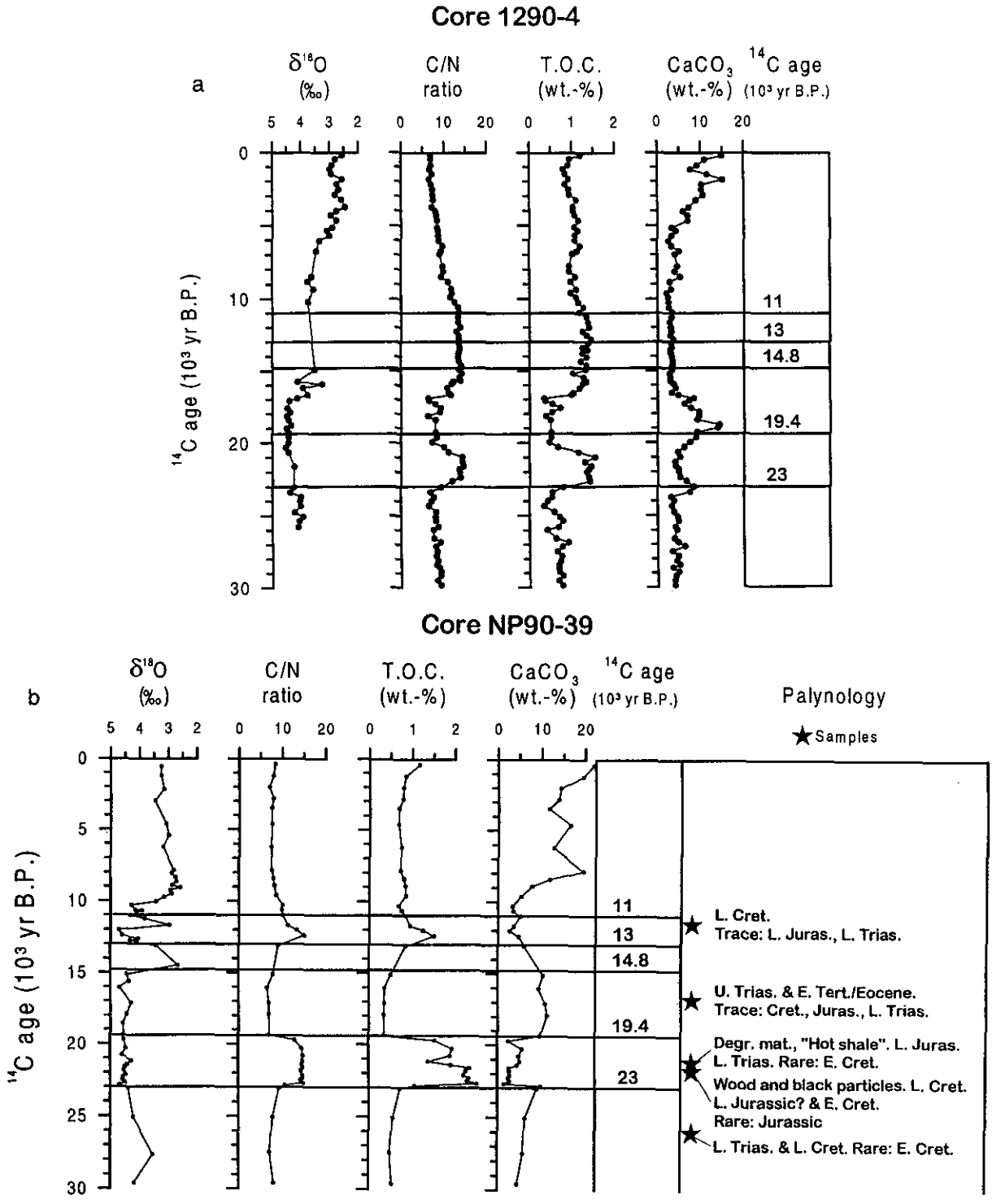

FIG. 4. Plot of $\delta^{18}O$, C/N-ratio, TOC, $CaCO_3$, and age estimates of reworked palynomorphs versus age. (a) 1290-4, (b) NP90-39, (c) NP90-12, (d) NP90-36, and (e) 1294-4.

3) as well as from the deep sea (Jones and Keigwin, 1988) show increased meltwater production that lasted until 13,000 ^{14}C yr B.P. On the upper slope, this period was marked by deposition of relatively high amounts of coarse sediment (dominated by clastic sedimentary grains), indicating increased rate of iceberg calving and input of rocks characteristic of the Svalbard region. In addition, a distinct increase in the C_{org} contents and C/N ratios (type B sediments) also suggests increased input of glacially eroded debris from Svalbard and/or the Barents Sea. This is supported by the palynomorphs which are dominated by Early Cretaceous assemblages characteristic of the Svalbard archipelago. A similar record is also observed in the upper slope core NP90-36 (Fig. 4d).

This early disintegration of the ice sheet is also recorded in

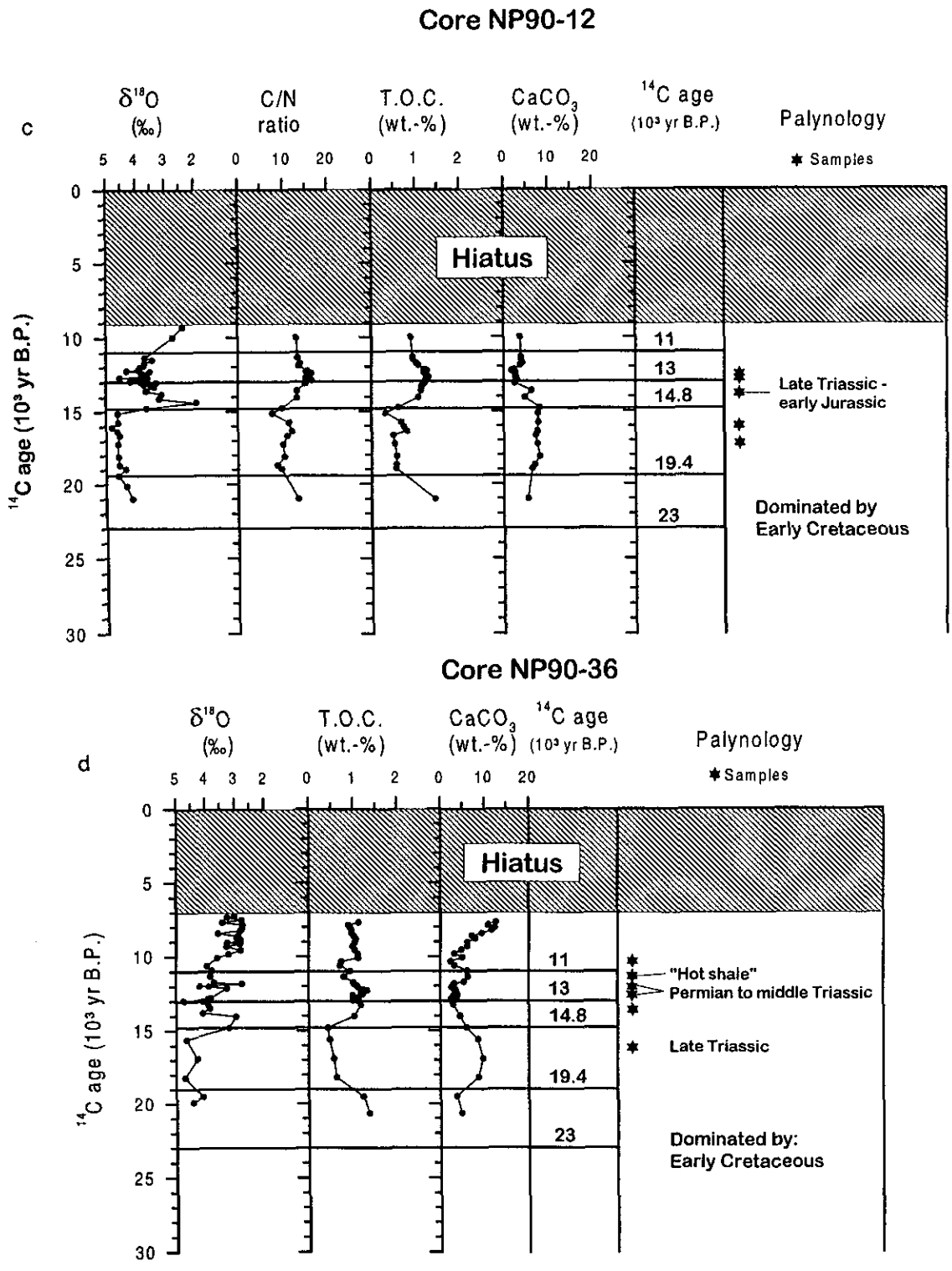

FIG. 4—*Continued*

the lower slope cores (e.g., NP90-39) by lower oxygen isotopes values. However, the period between 14,800 and 13,000 ^{14}C yr B.P. is characterized by low accumulation rates of fine-grained and ice-rafted sediment on the lower slope, compared with the more proximal core NP90-12 (Fig. 3d). Thus, sedimentation on the lower slope has not been directly affected by the initial phase of deglaciation. A possible explanation is that a strong coastal current may have kept the icebergs close to the shelf edge in a situation similar to that of modern East Greenland (Dowdeswell *et al.*, 1992), thereby inhibiting deposition on deeper part of the continental slope.

We have reasons to believe that there is a hiatus in shelf core NP90-21, above sediments dated 14,800–14,500 ^{14}C yr B.P. (Table 2). This level is marked by a thin (5-cm) pebbly lag

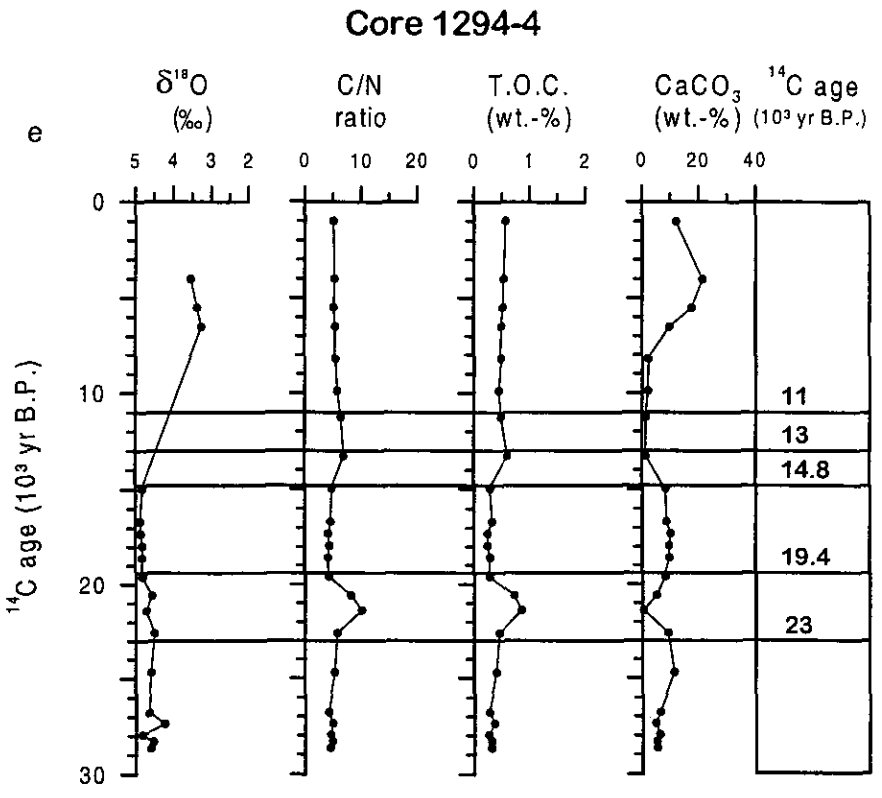

FIG. 4—*Continued*

5–19 cm above the till, probably caused by current activity. The sediments immediately above this level date to ca. 13,000 ^{14}C yr B.P., (Fig. 3d, Table 2). Thus, the period between 14,500 and 13,000 ^{14}C yr B.P., during which intensive iceberg rafting occurred on the upper slope (Figs. 3c and d), is not recorded on the shelf. The combination of light isotope values and high input of clasts originating from Svalbard on the slope indicates that this initial stage of ice recession from the outer shelf was characterized by melting of icebergs rather than direct meltwater runoff.

Our data indicate significant ice recession around 14,500 ^{14}C yr B.P. A wide-scale ice withdrawal is required in order to provide the high input of light isotopes. But since the ice did not leave the continental shelf off Spitsbergen before 12,500–11,500 ^{14}C yr B.P. (see below), we suggest that the marked meltwater signal reflects ice recession from the southern parts of the Barents Sea. This is in agreement with studies from the Barents Sea and the Norwegian-Greenland Sea (Jones and Keigwin, 1988; Sarnthein *et al.,* 1992; Elverhøi *et al.,* 1993).

13,000 to 11,000 ^{14}C yr B.P.

High accumulation rates on the slope as well as on the shelf have been measured in cores between 13,000 and 11,000 ^{14}C yr B.P. Accumulation rates on the order of 100–200 g/cm^2 · 1000 yr have been recorded both on the upper slope and outer shelf (Figs. 3c, 3d, and 3e). Furthermore, clasts of Late Paleozoic limestones from Svalbard appear for the first time in significant concentrations. Dates of shells from diamictons on the continental shelf, interpreted as till, indicate a glacier readvance that culminated shortly after 12,400 ^{14}C yr B.P. (J. I. Svendsen, unpublished data). This short-lived readvance is also reflected in outer shelf core NP90-21 (Fig. 3e) by increased IRD content, but not in upper slope cores. The glacier advance was followed by rapid retreat, and the outer part of Isfjorden was ice-free no later than 12,300 ^{14}C yr B.P. (Svendsen *et al.,* 1992). From previous onshore studies close to the mouth of Isfjorden, it is evident that the ice front was located inside Isfjorden after 12,000 ^{14}C yr B.P. (Mangerud *et al.,* 1992).

A second meltwater event occurred between approximately 12,500 and 11,500 ^{14}C yr B.P. (Figs. 3b and 3d). It, too, was marked by increased IRD input. However, in contrast to the first event, the second was associated with high bulk accumulation rates. Hence, we suggest that an extensive plume containing large amounts of suspended material, together with rapid calving, was established around 13,000 ^{14}C yr B.P.

The cores on the lower slope show a different deglacial signal than the upper slope cores. In NP90-39, the onset of high IRD about 12,000 ^{14}C yr B.P., which was associated with accumulation of crystalline grains, was followed by increased accumulation of clastic grains about 11,500 ^{14}C yr B.P. (Fig. 3b). The source of the latter is clearly the Svalbard–Barents Sea region, whereas the former may have originated from both the adjacent shelf and Fennoscandia. The combination of a well-defined peak of clastic grains, palynomorphs of a possible eastern Barents Sea provenance (Fig. 5, K2), and a well-defined meltwater signal suggest that final deglaciation of the Barents Sea began close to 12,000 ^{14}C yr B.P.

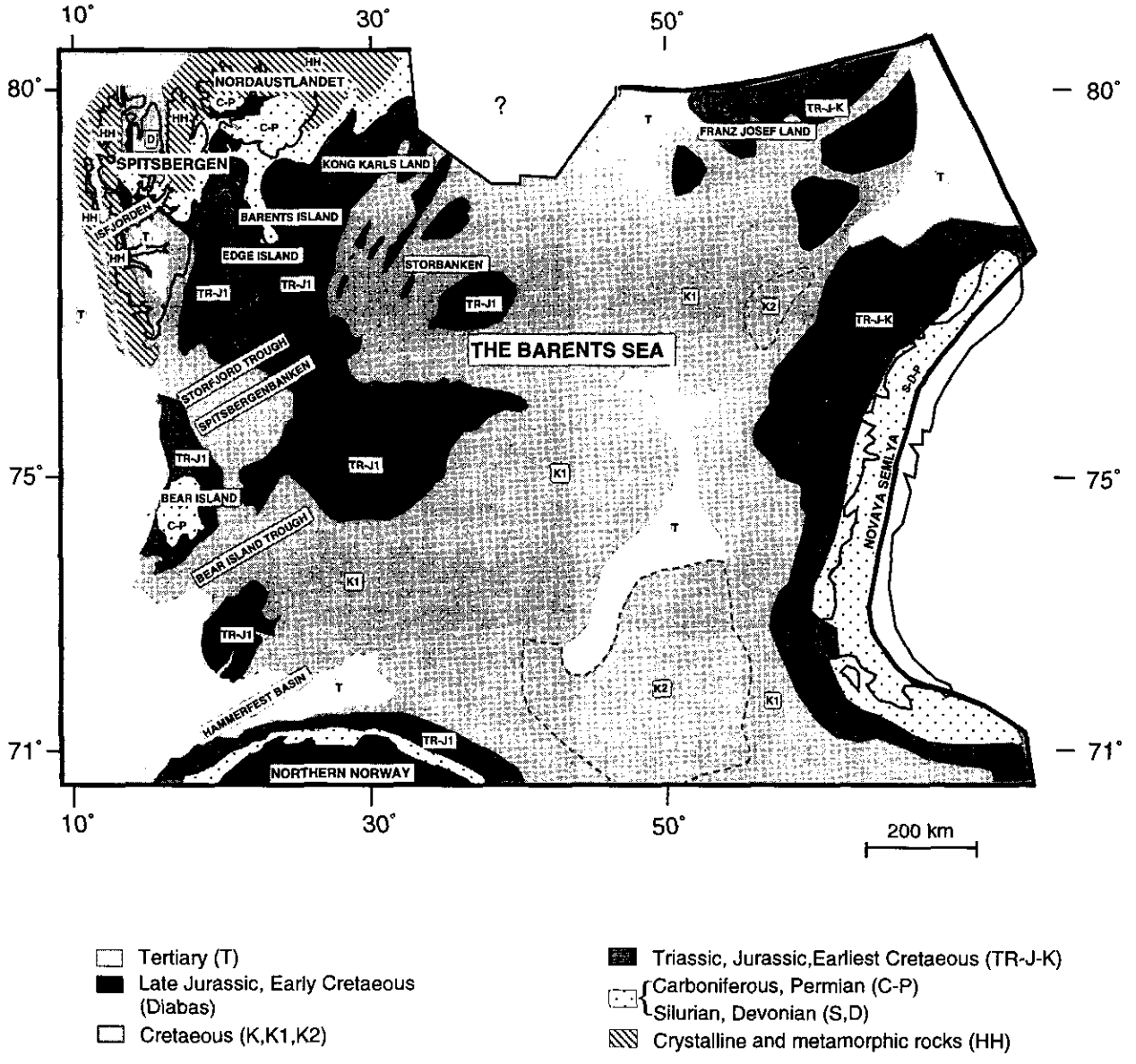

FIG. 5. Map showing the outcropping bedrock in the Barents Sea and on Svalbard (simplified from Sigmond (1992) and Johansen *et al.* (1992)).

The general low percentage of IRD and low C_{org} content in the slope sediments indicate that most of the shelf area in the northwestern Barents Sea was ice-free at that time.

11,000–9,500 ^{14}C yr B.P.

Although this period is poorly documented both in the slope and shelf cores, input of IRD to the shelf and slope decreased through this time (Fig. 3). Central Isfjorden is likely to have been ice-free, and large glaciers most likely existed in the inner fjord branches during the Younger Dryas interval (Mangerud *et al.*, 1992; Elverhøi *et al.*, 1995) when a significant portion of the glacialmarine sediments in Isfjorden were deposited (Elverhøi *et al.*, 1995). A series of dates from sea-floor sediments in the inner fjord branches demonstrate that high rates of glacialmarine sedimentation ended about 10,000 ^{14}C yr B.P. in Isfjorden, showing rapid disintegration of the remaining ice sheet immediately afterward (Elverhøi *et al.*, 1995). Warm conditions existed during early Holocene time, as reflected by relatively high $\delta^{18}O$ values (approximately 9500 ^{14}C yr B.P.) and high carbonate content (approximately 8000 ^{14}C yr B.P.).

CONCLUDING REMARKS

The growth of the marine-based Barents Sea Ice Sheet is strongly related to a fall in global sea level (Elverhøi *et al.*, 1993) and increased precipitation due to open marine conditions in the interval 27,000–23,000 ^{14}C yr B.P. (Hebbeln *et al.*, 1994). Such a concept has recently been modeled numerically, showing that the combination of sea level fall and increased precipitation, together with strongly reduced calving rate, favors the growth of the Barents Sea Ice Sheet (Siegert and Dowdeswell, 1995). Thus, the glacial history of the Svalbard

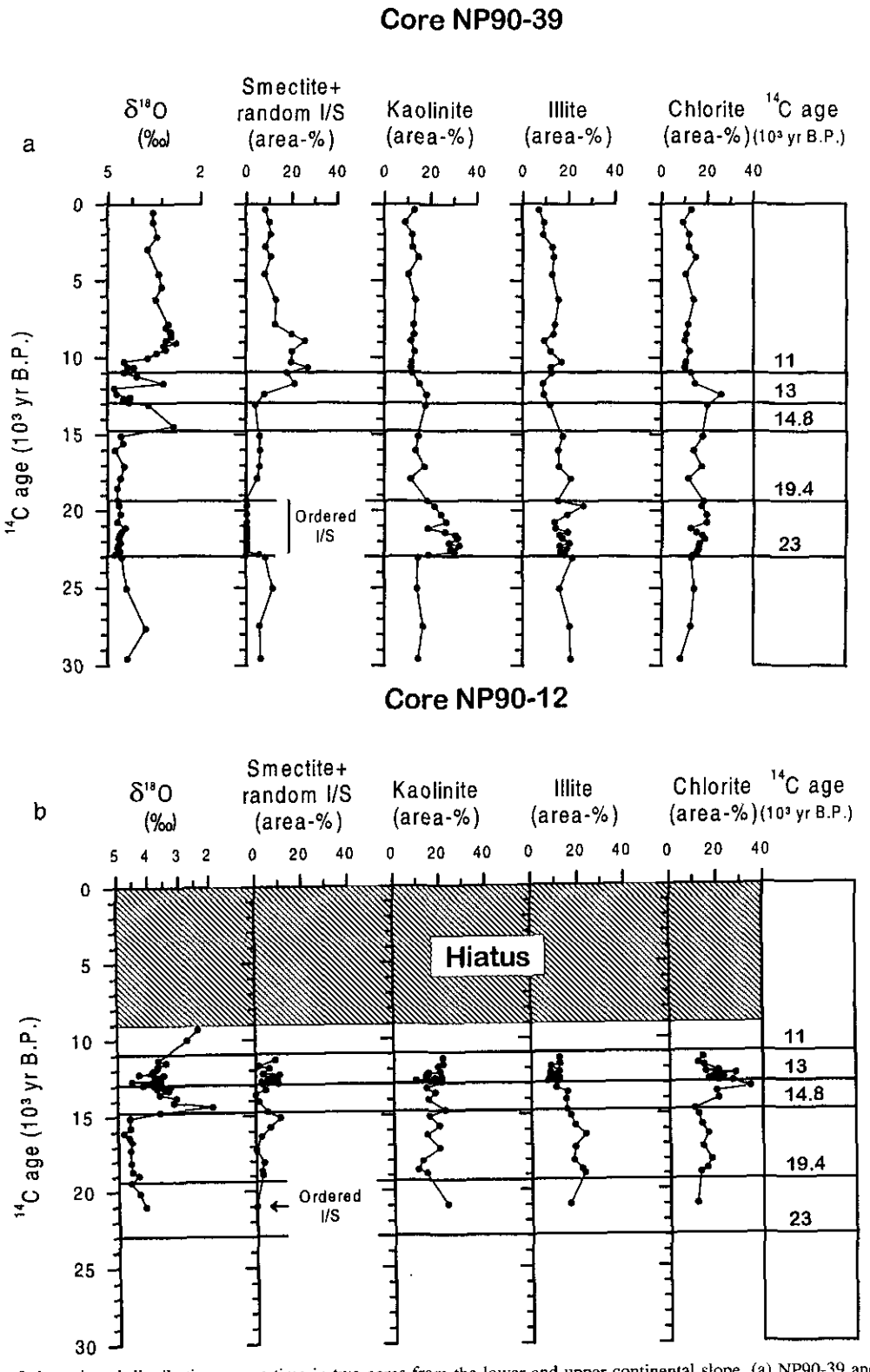

FIG. 6. Plot of clay mineral distribution versus time in two cores from the lower and upper continental slope. (a) NP90-39 and (b) NP90-12.

and northwestern Barents Sea seems not to correspond with the more recent published data from the Norwegian coastal and shelf waters where an ice advance about 30,000–22,000 ^{14}C yr B.P. has been advocated (Alm 1993; Sejrup *et al.*, 1994). The first period of high hemipelagic input to the Svalbard continental margin approximates the timing of one of the Heinrich events (Fig. 7). However, the event on the Svalbard margin is related to an expanding ice sheet and is not linked with massive

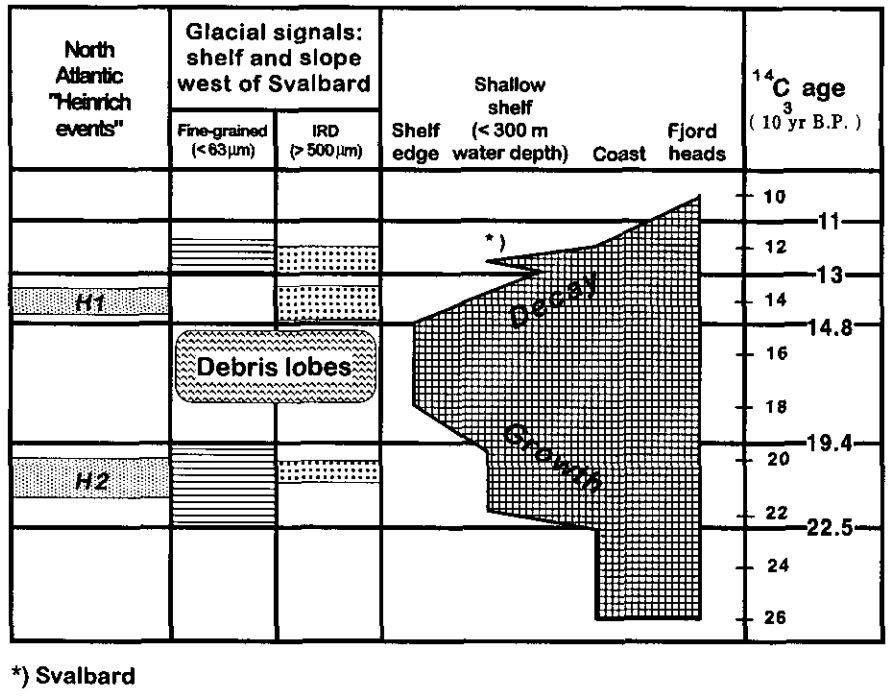

FIG. 7. Glaciation curve for the western Svalbard and northwestern Barents Sea ice sheets through the Late Weichselian glaciation.

discharge of icebergs and ice-sheet collapse, as proposed for the Heinrich events (Bond *et al.*, 1992; MacAyeal, 1993).

The last glacial maximum is the most complicated period to reconstruct from the Svalbard margin cores due to apparently conflicting data. Based on a large number of glacial-geologic features, the entire Barents Sea and the shelf west of Svalbard appears to have been covered by grounded ice during this period (Vorren *et al.*, 1988; Svendsen *et al.*, 1992; Elverhøi *et al.*, 1993). However, no sign of glacier activity on the adjacent shelf was found in the slope cores. Based on sediment cores from the Isfjorden Fan, which is the main depocenter of the Isfjorden drainage area (Elverhøi *et al.*, 1995), debris flow activity is likely to have occurred during this period. Recent results from the Bear Island Fan also indicate high sediment discharge to the slope by debris flows during glacial maximum (Laberg and Vorren, 1995). Based on mass calculation and sediment build-up of the Isfjorden Fan (Elverhøi *et al.*, 1995) we think it plausible that the ice was located on the shelf edge for at least several thousand years. Thus, an ice advance to the shelf edge may have occurred ca. 18,000 ^{14}C yr B.P., where it remained for at least 3000 years (Fig. 7).

Deglaciation occurred in two steps, the first starting immediately after 15,000 ^{14}C yr B.P. and characterized by ice recession from the outer shelf off Isfjorden, in addition to an extensive ice recession of the southwestern Barents Sea. The pronounced oxygen isotope peak around 14,500 ^{14}C yr B.P., combined with evidence of intensive ice-rafting on the upper slope, suggests that the light isotope values are related mainly to the melting of icebergs. Although the initial phase of deglaciation of the Svalbard-northwestern Barents Sea Ice Sheet may be comparable with Heinrich event H1, we do not yet know if this discharge was caused by internal instability of the ice sheet or due to external forcing, e.g., by a rise of sea level (e.g., Jones and Keigwin, 1988).

In contrast to the first peak, the second injection of light isotopes, which started just after 13,000 ^{14}C yr B.P., is associated with a major influx of fine-grained sediment to the shelf and upper slope, indicating a major release of meltwater from the ice sheet. Thick glacialmarine sediments, interpreted as glacier-proximal deposits, at 300 m depth in the Barents Sea (Elverhøi *et al.*, 1993), support the idea that the later period of deglaciation was associated with subglacial drainage and extensive release of sediments from a turbid plume. As a result of this second stage of ice recession, the central Barents Sea became deglaciated (Fig. 7). During this period, about 12,500 ^{14}C yr B.P., a minor readvance of the ice occurred on the shelf west of Svalbard. Evidence of a similar event is also observed along the Norwegian coastal waters (Mangerud *et al.*, 1979; Vorren *et al.*, 1988).

Although the phases of enhanced terrigenous input along the Spitsbergen margin correlate with North Atlantic Henrich events H1 and H2, the differences in the stability of the Barents and Laurentide ice sheets do not suggest a common forcing.

ACKNOWLEDGMENTS

This study is a contribution to the project PONAM (Polar North Atlantic Margin: Late Cenozoic Evolution). The Norwegian contribution is financially supported by Statoil, Norsk Hydro, The Norwegian Petroleum Directorate, Saga Petroleum, and the Research Council of Norway (NFR). Sediment cores were acquired by the Norwegian Polar Research Institute and the Alfred Wegner Institute for Polar and Marine Research in Bremerhaven. Tor Bjærke, StratLab, Norway is acknowledged for analyzing the palynomorphs and Martin Siegert and Julian Dowdeswell for valuable comments made to the manuscript.

REFERENCES

Alm, T. (1993). Øvre Æråsvatn—Palynostratigraphy of a 22,000 to 10,000 BP lacustrine record on Andøya, northern Norway. *Boreas* **22,** 171–188.

Andersen, E. S., Solheim, A., and Elverhøi, A. (1994). Development of a glaciated arctic continental margin: Exemplified by the western margin of Svalbard. *In* "International Conference on Arctic Margins (ICAM): Proceedings, Anchorage, Alaska, 1992" (D. K. Thurston and K. Fujita, Eds.), pp. 155–160. U.S. Department of the Interior, Mineral Management Service, Alaska Outer Continental Shelf Region, OCS Study, MMS 94-0040.

Andersen, E. S. (1995). "Sedimentary Development of Glaciated Margins: The Svalbard Margin and the Northern North Sea During the Plio- and Pleistocene." Ph.D dissertation, University of Oslo.

Bjærke, T. (1993). "Palynonlogical Analyses of Rock Fragments from the Svalbard margin." Unpublished report, University of Oslo. 15 pp.

Bjørlykke, K., Bue, B., and Elverhøi, A. (1978). Quaternary sediments in the northwestern part of the Barents Sea and their relation to the underlying Mesozoic bedrock. *Sedimentology* **25,** 227–246.

Bond, G., Heinrich, H., Broecker, W., Labeyrie, L., McManus, J., Andrews, J., Huon, S., Jantschik, R., Clasen, S., Simet, C., Tedesco, K., Klas, M., Bonani, G., and Ivy, S. (1992). Evidence for massive discharge of icebergs into the North Atlantic ocean during the last glacial period. *Nature* **360,** 245–249.

Dokken, T. (1995). "Paleoceanographic Changes during the Last Interglacial–Glacial Cycle from the Svalbard-Barents Sea Margin: Implications for Ice-Sheet Growth and Decay." Ph.D. dissertation, University of Tromsø.

Dowdeswell, J. A., and Dowdeswell, E. K. (1989). Debris in icebergs and rates of glaciomarine sedimentation: Observations from Spitsbergen and a simple model. *Journal of Geology* **97,** 221–231.

Dowdeswell, J. A., Whittington, R. J., and Hodgkins, R. (1992). The size, frequencies and freeboard of east Greenland icebergs observed using ship radar and sextant. *Journal of Geophysical Research* **97,** 3515–3528.

Ehrmann, W., and Thiede, J. (1985). History of Mesozoic and Cenozoic sediment fluxes to the North Atlantic Ocean. *Contribution Sedimentology* **15,** 109.

Elverhøi, A., Pfirman, S. L., Solheim, A., and Larsen, B. B. (1989). Glaciomarine sedimentation on epicontinental seas—As exemplified by the northern Barents Sea. *Marine Geology* **85,** 59–66.

Elverhøi, A., Fjeldskaar, W., Solheim, A., Nyland-Berg, M., and Russwurm, L. (1993). The Barents Sea—A model of it's growth and decay during the last ice maximum. *Quaternary Science Review* **12,** 863–873.

Elverhøi, A., Svendsen, J. I., Solheim, A., Andersen, E. S., Milliman, J. D., Mangerud, J., and Hooke, LeB. R. (1995). Late Quaternary sediment yield from the high Arctic Svalbard area. *Journal of Geology* **103,** 1–17.

Emerson, S., and Hedges, J. I. (1988). Processes controlling the organic carbon content of open ocean sediments. *Paleoceanography* **3,** 621–634.

Hebbeln, D. (1992). Weichselian glacial history of the Svalbard area: Correlating the marine and terrestrial records. *Boreas* **21,** 295–304.

Hebbeln, D., Dokken, T., Andersen, E. S., Hald, M., and Elverhøi, A. (1994). Moisture supply for northern ice-sheet growth during the Last Glacial Maximum. *Nature* **370,** 357–360.

Hopkins, T. T. (1991). The GIN Sea—A synthesis of its physical oceanography and literature review 1972–1985. *Earth-Science Reviews* **30,** 175–318.

Hughes, T. J. (1992). Theoretical calving rates from glaciers along ice walls grounded in water of variable depths. *Journal of Glaciology* **38,** 282–294.

Johansen, S., Ostisty, B. K., Birkeland, Ø., Fedorovsky, V. N., Bruun Christensen, O., Cheredeev, S. I., Ignatenko, E. A., and Margulis, L. S. (1992). Hydrocarbon potential in the Barents Sea region: Play distribution and potential. *In* "Arctic Geology and Petroleum Potential" (T. O. Vorren, A. Bergsager, Ø. A. Dahl-Stamnes, E. Holter, B. Johansen, E. Lie, and T. B. Lund, Eds.), Norsk Petroleumsforening/NPF Special Publication, pp 273–320, Elsevier, Amsterdam.

Jones, G. A., and Keigwin, L. D. (1988). Evidence from Fram Strait (78° N) for early deglaciation. *Nature* **336,** 56–59.

MacAyeal, D. R. (1993). Binge/purge oscillations of the Laurentide Ice Sheet as a cause of the North Atlantic's Heinrich Events. *Paleoceanography* **8,** 775–784.

Mangerud, J., Larsen, E., Longva, O., and Sønstegaard, E. (1979). Glacial history of western Norway 15,000–10,000 B.P. *Boreas* **8,** 179–187.

Mangerud, J., Bolstad, M., Elgersma, A., Helliksen, D., Landvik, J. Y., Lønne, I., Lcyke, A. K., Salvigsen, O., Sandahl, T., and Svendsen, J. I. (1992). The Last Glacial Maximum on Spitsbergen, Svalbard. *Quaternary Research* **38,** 1–31.

Mangerud, J., and Gulliksen, S. (1975). Apparent radiocarbon ages of recent marine shell from Norway, Spitsbergen, and Arctic Canada. *Quaternary Research* **5,** 263–273.

Mangerud, J., and Svendsen, J. I. (1992). The last interglacial–glacial period on Spitsbergen, Svalbard. *Quaternary Science Review* **11,** 633–664.

Pearson, M. J. (1990). Clay mineral distribution and provenance in Mesozoic and Tertiary mudrocks of the Moray Firth and northern North Sea. *Clay Minerals* **23,** 519–541.

Pfirman, S. L., Wollenburg, I., Thiede, J., and Lange, M. A. (1989). Lithogenic sediment on Arctic pack ice: Potential aeolian flux and contribution to deep sea sediments. *In* "Paleoclimatology and Paleometeorology: Modern and Past Patterns of Global Atmospheric Transport" (M. Leinenand and M. Sarnthein, Eds.), NATO ASI Series C 282, pp. 463–493. Kluwer, Dordrecht.

Sarnthein, M., Jansen, E., Arnold, M., Duplessy, J. C., Erlenkeuser, H., Flatøy, A., Veum, T., Vogelsang, E., and Weinelt, M. S. (1992). d^{18} O time-reconstructions of meltwater anomalies at termination I in the North Atlantic between 50 and 80°N. *In* "The Last Deglaciation: Absolute and radiocarbon Chronologies" (E. Bard and W. S. Broecker, Eds.), NATO ASI Series 2, pp. 1–13, Springer, Berlin.

Sejrup, H. P., Haflidason, H., Aarseth, I., King, E., Forsberg, C. F., Long, D., and Rokoengen, K. (1994). Late Weichselian glaciation history of the northern North Sea. *Boreas* **3,** 1–13.

Siegert, M. J., and Dowdeswell, J. A. (1995). Modelling ice sheet sensitivity to Late Weichselian environment in the Svalbard-Barents Sea region. *Journal of Quaternary Science* **10,** 33–43.

Sigmond, E. M. O. (1992). "Bedrock Map of Norway and Adjacent Ocean Areas," Scale 1: 3 million. Geological Survey of Norway.

Solheim, A., Russwurm, L., Elverhøi, A., and Nyland-Berg, M. (1990). Glacial geomorphic features: Direct evidence for grounded ice in the northern Barents Sea and implications for the pattern of deglaciation and late glacial sedimentation. *Geological Society of London Special Publication* **53,** 253–268.

Spielhagen, R. F. (1991). Die Eisdrift in der Fram Strasse während der letzen 200,000 Jahre. *Geomar Report* **4,** 1–144. [Kiel]

Svendsen, J. I., Mangerud, J., Elverhøi, A., Solheim, A., and Schüttenhelm, R. T. E. (1992). The Late Weichselian glacial maximum on western Spitsbergen inferred from offshore sediment cores. *Marine Geology* **104,** 1–17.

Vinje, T. (1985). Drift, composition, morphology and distribution of the sea ice fields in the Barents Sea. *Norsk Polarinstitutt Skrifter* **179C,** 1–26.

Vorren, T. O., Hald, M., and Lebesbye, E. (1988). Late Cenozoic environment in the Barents Sea. *Paleoceanography* **3,** 601–612.